

# Inoculum Dose, Diversity, Dispersal, and Damage: Simulating Optimal Economic Control of an Aerially-Dispersed Plant Pathogen

Joshua F. Pedro<sup>1</sup>, Sharmodeep Bhattacharyya<sup>2</sup>, Shirshendu Chatterjee<sup>1</sup>,  
Thomas L. Marsh<sup>3</sup>, Jae Young Hwang<sup>4</sup>, and David H. Gent<sup>4,\*</sup>

<sup>1</sup>Department of Mathematics, City University of New York, NY 10031

<sup>2</sup>Department of Statistics, Oregon State University, Corvallis, OR 97331

<sup>3</sup>School of Economic Sciences, Washington State University, Pullman, WA  
99163

<sup>4</sup>U.S. Department of Agriculture-Agricultural Research Service, Forage  
Seed and Cereal Research Unit, Corvallis, OR 97331

\*Corresponding author: David H. Gent [dave.gent@usda.gov](mailto:dave.gent@usda.gov)

## Abstract

Plant pathogens that disperse by airborne propagules may cause damage that extends beyond the borders of individual fields. Developing sound management strategies, therefore, requires consideration of heterogeneity in pathogen transmission, the effectiveness of control measures, host susceptibility and pathogen virulence, and the resulting economic outcomes that scale up at the regional level with coordinated management. We use hop powdery mildew as a motivating pathosystem to develop a coupled epidemiological-economic model to enable simulation of the impact of epidemic conditions and coordinated management interventions on profitability. This pathosystem is a well-suited case study because disease development may be limited by primary inoculum and fungicide applications, yet the pathogen can spread via long-distance dispersal between fields and rapidly damage both crop yield and quality. We parameterized the model using data collected from a census sample of commercial hop yards in Oregon during 2014 to 2017, including the monthly incidence of plants with powdery mildew, fungicides applied by growers, and estimated revenue depending on how the incidence of diseased hop cones affects yield and the likelihood of crop devaluation. We show that conditions in the early stages of epidemics related to primary inoculum dose, pathogen diversity, and the intensity of management intervention interact and determine the optimal regional

control strategy. As the likelihood of primary infection increases, due to either the dose of primary inoculum or virulence of the pathogen population, mean profitability decreases. These effects are most pronounced when primary infection occurs in the yards that are most central in the disease transmission network. The choice of how many fungicide applications to make in response to initial infection has little effect on profitability when the primary inoculum is relatively infrequent. However, as primary inoculum increases, targeted fungicide applications made in the early stages of epidemics are essential for maximizing profitability region-wide. These principles hold across a range of market demand scenarios that change crop quality standards, even though relative profit losses increase under low demand conditions. Our analysis addresses a multifaceted challenge in agricultural disease management where epidemic control decisions must account for interactions between pathogen biology, management practices, market conditions, and regional-scale disease transmission. This research provides a framework for formally understanding factors that influence the cost of disease in complex agricultural systems where pathogens disperse across management units.

**Keywords:** plant disease, pathogens, epidemiology, economic impacts, disease management, landscape-scale

<b>Contents</b>	50
<b>1 Introduction</b>	<b>4</b> 51
<b>2 Material and Methods</b>	<b>7</b> 52
2.1 Study system . . . . .	7 53
2.2 Biological data acquisition . . . . .	8 54
2.3 Pesticide use and costs . . . . .	8 55
2.4 General modeling approach . . . . .	9 56
2.5 Submodels . . . . .	9 57
2.5.1 Epidemic network model . . . . .	9 58
2.5.2 Economic model . . . . .	11 59
2.5.3 Parameter estimation . . . . .	14 60
<b>3 Simulation experiments</b>	<b>15</b> 61
3.1 Summary of simulation parameters . . . . .	17 62
<b>4 Results</b>	<b>17</b> 63
4.1 Parameter estimates for epidemic model . . . . .	17 64
4.2 Simulation experiments . . . . .	18 65
4.2.1 Impact of initial inoculum dose . . . . .	18 66
4.2.2 Effect of pathogen diversity . . . . .	19 67
4.2.3 Influence of degree-centrality of initial inoculum . . . . .	19 68
4.2.4 Market demand conditions . . . . .	19 69
<b>5 Discussion</b>	<b>20</b> 70
5.1 Early intervention and threshold effects . . . . .	20 71
5.2 Market sensitivity and economic injury level paradigms . . . . .	22 72
5.3 Study limitations and future directions . . . . .	23 73
<b>6 Appendix</b>	<b>23</b> 74
6.1 Parameter estimates . . . . .	24 75
6.2 Poisson Regression Model for Fungicide Applications . . . . .	24 76
6.3 Supplementary results . . . . .	25 77
6.4 Sensitivity analysis . . . . .	25 78

# 1. Introduction

79

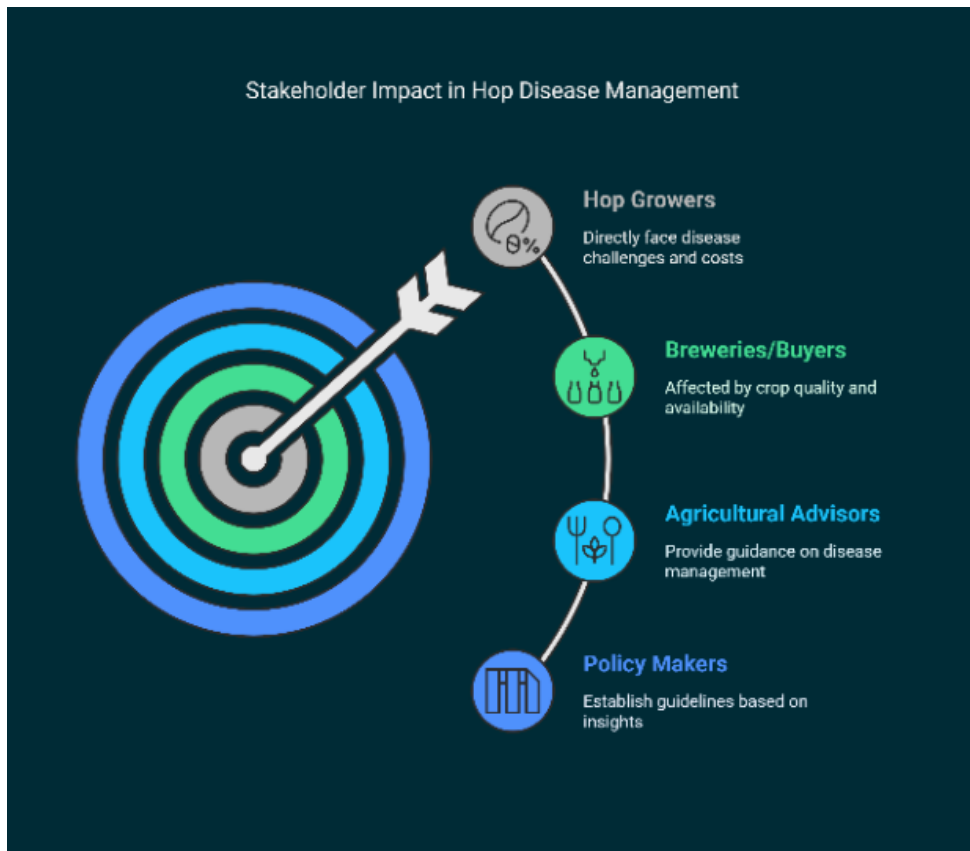


Figure 1: Stakeholder impact network of disease management in the motivating hop powdery mildew pathosystem. This diagram depicts the interconnected relationships among key stakeholders affected by disease management decisions, including hop growers (who directly face disease challenges and costs), breweries/buyers (affected by crop quality and availability), agricultural advisors (who provide guidance on disease management), and policy makers (who establish guidelines based on research insights).

There is increasing scrutiny of pesticides in agriculture and a need to develop management strategies and policies that reduce inputs while maintaining productivity and profitability (de Waard et al., 1993; Pimentel, 2005). Disease management efforts are most often directed at the scale of individual fields or farms, but plant pathogens do not respect management units or jurisdictional boundaries (Gilligan, 2008). Management may be suboptimal or ineffective when not properly matched to the scale of pathogen dispersal (Gilligan et al., 2007). The relative importance of inoculum produced endogenously within a given field or exogenously in other locations may dictate the mitigation strategies and the need for collective action in the form of area-wide management (Irwin, 1999).

Foundational theory in plant disease epidemiology suggests that mitigation efforts that reduce primary inoculum only delay epidemics, with the effect being inversely proportional to epidemic velocity (van der Plank, 1963). Yet, a number of empirical studies and modeling suggest that early intervention is critical for containing the spread of dis-

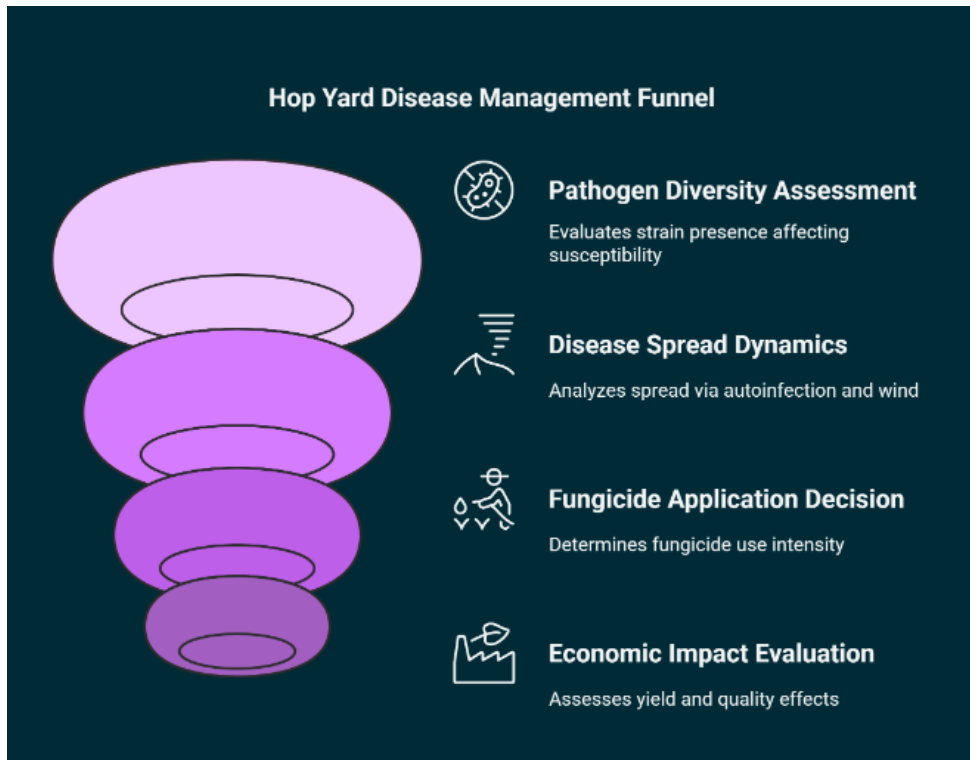


Figure 2: **Conceptual framework for disease management in the motivating pathosystem.** This funnel diagram illustrates the multi-stage decision-making process in disease management, showing the sequential evaluation of pathogen diversity assessment, disease spread dynamics, fungicide application decisions, and economic impact evaluation. Each stage represents a key component of the integrated epidemiological-economic model developed in this study.

ease outbreaks (Cunniffe, Stutt et al., 2015; Fraser et al., 2004). Epidemics caused by pathogens capable of long-distance dispersal appear sensitive to the conditions in the initial outbreak area (Estep et al., 2014; Severns & Mundt, 2022). Final epidemic severity may depend on the size of the initial focus, pattern of initial inoculum, proportion of susceptible hosts in the population, and connectivity to other susceptible hosts (Ojiambo et al., 2017; Severns et al., 2014). The importance of these factors may depend sensitively on parameters controlling pathogen transmission and stochasticity in the earliest stages of an epidemic (Xu & Ridout, 1998). Concrete recommendations for control strategies also depend on the relative effectiveness and costs of controls (Margosian et al., 2009).

The need for modeling to explicitly express processes and current understanding of a system is clear (Lofgren et al., 2014; Pautasso et al., 2010), yet linking epidemiological models to crop damage and economic outcomes when pathogens potentially disperse over long distances is a challenging problem (Cunniffe, Koskella et al., 2015). The motivating pathosystem for the research we present, hop powdery mildew, engenders many of these challenging aspects. The disease is caused by the fungus *Podosphaera macularis* and remains one of the most difficult and costly problems affecting hop producers in the western U.S. and other production regions. Success in breeding cultivars resistant to the disease has been met by the emergence of strains of the fungus that can overcome

host resistance when the said resistance is broadly deployed in the landscape. Therefore, 112  
management still relies heavily on cultural practices that reduce inoculum density and 113  
fungicides to slow the rate of disease progression. 114

This pathosystem has several biological and economic attributes that make it an ex- 115  
emplar for developing the modeling framework we propose herein, and also broadly of 116  
interest for other aerially-dispersed plant pathogens in complex social-ecological systems. 117

First, the causal pathogen is an obligate biotroph with a host range limited to the plant 118  
family Cannabaceae, with hop being the dominant and most important host cultivated 119  
at the time of these studies. Consequently, it is possible to infer disease transmission 120  
between yards because other sources of inoculum are trivial. Further, this system is 121  
amenable to modeling dispersal between yards as *P. macularis* exhibits annual cycles of 122  
emergence, colonization, and extinction. The fungus persists from season to season in 123  
the Pacific Northwestern U.S. only in association with living host tissue, provisioned by 124  
infected crown buds, due to the absence of the sexual stage of the pathogen in this region. 125  
Bud infection and overwintering of the pathogen lead to highly focal infections owing to 126  
the emergence of heavily infected shoots in spring, the so-called flag shoots, which occur 127  
at a low frequency in commercial hop yards. From these focal infections, *P. macularis* 128  
disperses via wind and readily spreads within the network of hop yards to create regional 129  
epidemics. At the end of the cropping season, the pathogen becomes locally extinct in 130  
most yards due to its low overwintering survival. Thus, a new realization of the disease 131  
development and transmission process can be observed annually. 132

Pathogenic variation is common in pathogens across plant and animal hosts and has 133  
important implications for the dynamics of disease transmission and severity. This is 134  
especially relevant in agricultural systems where R-gene-mediated resistance is deployed 135  
and creates a mosaic of resistant and susceptible hosts. Host resistance to powdery mildew 136  
is commercially available in hop and multiple pathogenic variants (strains) exist in *P. 137*  
*macularis* in certain populations. As hop plants are long-lived perennials, relatively stable 138  
patterns of resistant and susceptible cultivars are present in the landscape. 139

The pathosystem is of further interest because powdery mildew may cause economic 140  
losses by reducing both yield and crop quality. This is a common scenario in many 141  
agricultural systems, particularly for crops marketed directly to consumers with cosmetic 142  
value. In these situations, the financial loss incurred by the grower may be linked in 143  
complex ways to market demand. Indeed, this is the situation with hops and powdery 144  
mildew because the disease may reduce brewing value and cause conspicuous visual defects 145  
from degraded cone color. For this reason, growers apply fungicides repeatedly during the 146  
season with the goal of minimizing inoculum pressure for the critical cone phase of the 147  
disease. Fungicide applications for powdery mildew may occur over a period of multiple 148  
months to minimize foliar infections in spring and then later in summer to minimize cone 149  
infection. Thus, growers must make multiple decisions on when to begin treatment and 150  
how intensively to treat. 151

Adding even more uncertainty, hops are sold almost entirely through marketing contracts that stipulate quality standards, usually with vague or subjective quality standards. Contracting is conducted for numerous agricultural commodities, and in 2017 21 percent of total U.S. crop production was under a contract agreement. Price risk reduction is stated as a major incentive for contracting. The potential for crop devaluation or, in the worst case, rejection, may substantially affect disease management choices since the producer assumes firstly the risk of crop damage and secondly the penalty for failing on a contractual obligation. We expect that optimal disease control strategies may therefore be sensitive to contract structure when crop value or saleability is inseparably linked to crop quality metrics. Furthermore, the optimal control strategy may depend on practices in other fields and other farms, given the potential for long-distance dispersal of the pathogen.

Motivated by this pathosystem, we draw upon an exceptionally rich data set collected from a census sample of hop yards in Oregon over a four-year period for our analyses. We formulate an epidemiological model for the development and spread of powdery mildew at the regional level, including the effect of fungicides applied in a field of interest and all other potential source fields. We couple the epidemiological model to an economic model of expected revenue and costs associated with disease management, devaluation or rejection due to quality defects, and market conditions (Figures 1 and 2). We then simulate varying conditions of the initial phases of epidemics related to primary inoculum dose, pathogen diversity, centrality in the transmission network of fields, and management intervention to identify control strategies that maximize profit under varying market demand scenarios.

## 2. Material and Methods

### 2.1 Study system

Our study system is the hop production region in western Oregon. Oregon is one of the leading hop producing regions in the U.S. and commercial production is concentrated in a few counties in the Willamette Valley in the western portion of the state. Hop powdery mildew was first confirmed in the field in Oregon in 1998 and has occurred annually each year since then. Historically, powdery mildew has tended to occur most regularly and most severely in production regions in the eastern extent of the Willamette Valley, presumably due to the frequency of overwintered inoculum and subsequent dispersal from the resultant disease foci (Mahaffee & Stoll, 2016). We intentionally focused on hop farms in the eastern production regions for data acquisition. The diversity of cultivars and production practices in this region are summarized elsewhere (Thompson et al., 2016).

## 2.2 Biological data acquisition

186

We obtained monthly data on the incidence of plants with powdery mildew or primary 187  
infection (i.e., occurrence of a flag shoot) from a census survey of hop yards. Disease 188  
assessments were conducted monthly from April to July during each of 2014 to 2017. 189  
For brevity, a summary of the disease assessment methods is provided here; a complete 190  
description of the methods is given in the referenced work (Bassanezi et al., 2013). There 191  
were 8 to 10 farms sampled per year, all within Marion County, Oregon, with a max- 192  
imum distance between yards of 26 km. After cleaning, data were available for 99 yards 193  
assessed in 2014, 113 in 2015, 116 in 2016, and 122 in 2017. All cultivars were eval- 194  
uated, independent of their susceptibility to powdery mildew. The incidence of plants with 195  
powdery mildew was assessed using a modification of cluster sampling methods described 196  
previously (Filho et al., 2016). 197

As noted previously, there are multiple pathogenic strains of *P. macularis* that differ in 198  
their ability to cause disease on hop plants with specific resistance genes (R-genes). Two 199  
strains of the pathogen were relevant at the time of the field surveys and are differentiated 200  
based on their ability to cause disease on plants with a resistance termed R6. The presence 201  
of R6 resistance is analogous to immunization that provides complete, but strain-specific, 202  
protection from disease. The presence of R6 in hop plants provides resistance to powdery 203  
mildew only when the pathogen lacks a corresponding virulence (V). For shorthand, we 204  
refer to strains that cannot infect plants with R6 resistance as non-V6-virulent. Other 205  
strains of the pathogen may infect susceptible plants that lack R6, but importantly, can 206  
also infect plants that possess R6. These strains are dubbed V6-virulent. V6-virulent 207  
strains are promiscuous in the yards they may affect, as they infect hop cultivars that 208  
both possess or do not possess R6, analogous to a vaccine-evasive strain of a pathogen. 209

When we detected powdery mildew in a given hop yard, it was necessary to match 210  
the strain of the pathogen present to potential yards where the pathogen could disperse 211  
to cause disease. Therefore, the initial strain of the pathogen present was determined to 212  
be V6-virulent or non-V6-virulent using bioassays as described previously. 213

## 2.3 Pesticide use and costs

214

We obtained pesticide application records from each grower for all yards sampled during 215  
2014 to 2017 and interrogated their records to determine the timing and dosage of ap- 216  
plications of herbicides, fungicides with activity against powdery mildew, and adjuvant 217  
additives. Herbicides were of relevance because they are used in cultural practices to mod- 218  
erate powdery mildew (Gent et al., 2013, 2016, 2018). We did not consider insecticides 219  
or miticides because these were not directly relevant for the present analysis of powdery 220  
mildew. We then estimated the January 2022 real costs of the relevant pesticides and 221  
adjuvants applied by requesting price quotes for each product from each of three vendors 222  
in western Oregon that service hop producers as described in the referenced work. We 223

estimated real prices using January 2022 as the base by adjusting the nominal price by 224  
the producer price index for farm products for each year available from the U.S. Bureau 225  
of Labor Statistics, and then averaged over all available years to derive a single real price 226  
per unit. 227

## 2.4 General modeling approach 228

We introduce a linked epidemiological-economic statistical model of epidemic development 229  
and apply this model to hop powdery mildew to simulate economic outcomes due to disease 230  
management costs and crop damage from direct losses in yield and quality defects. The 231  
epidemic model contains both stochastic and deterministic components to estimate the 232  
development of the foliar phase of powdery mildew originating from initial occurrences 233  
of *P. macularis* via bud perennation, autoinfection at the scale of individual hop yards 234  
from inoculum endogenous to a given yard, and exogenous inoculum dispersed from other 235  
yards in the region. The population moment estimate of the incidence of plants with 236  
powdery mildew is derived from a function of the probability of a plant being diseased, 237  
as moderated by fungicide use. Profits are the summation of revenue and fixed and 238  
variable costs as influenced by fungicide inputs, and yield and crop devaluation due to 239  
quality defects as a function of disease incidence. External drivers are inputs of wind 240  
data, fungicide use, and initializing values of the probability of initial (primary) infection 241  
due to bud perennation, expected crop yield in the absence of disease, and price per unit 242  
of yield. The model is spatially explicit at the scale of individual hop yards and uses the 243  
actual location and size of hop yards in the data set for a representative year; there is no 244  
attempt to account mechanistically for focus development or disease spread within hop 245  
yards. 246

We use the linked models to simulate profit levels resulting from varying epidemic 247  
conditions. Concretely, these conditions were related to initial infection frequency, patho- 248  
genic diversity of the initial strain of the pathogen, the location of the initial infections, 249  
and the number of fungicide applications made in the first month of the epidemic. We 250  
aggregate responses from individual yards to scale to the regional population of yards. We 251  
then ran each simulation scenario under three market demand scenarios to understand 252  
the sensitivity of the results to market conditions. 253

## 2.5 Submodels 254

### 2.5.1 Epidemic network model 255

An individual hop yard is considered a node in a network of yards in the spatial extent of 256  
interest (Figure 3). Disease status of a yard in a given month is a nonlinear function of 257  
its disease incidence in the preceding month, susceptibility to two races of *P. macularis*, 258  
and disease spread from other nodes as influenced by their disease incidence and area 259  
(source strength), distance apart, and wind run in the preceding month. We expanded 260

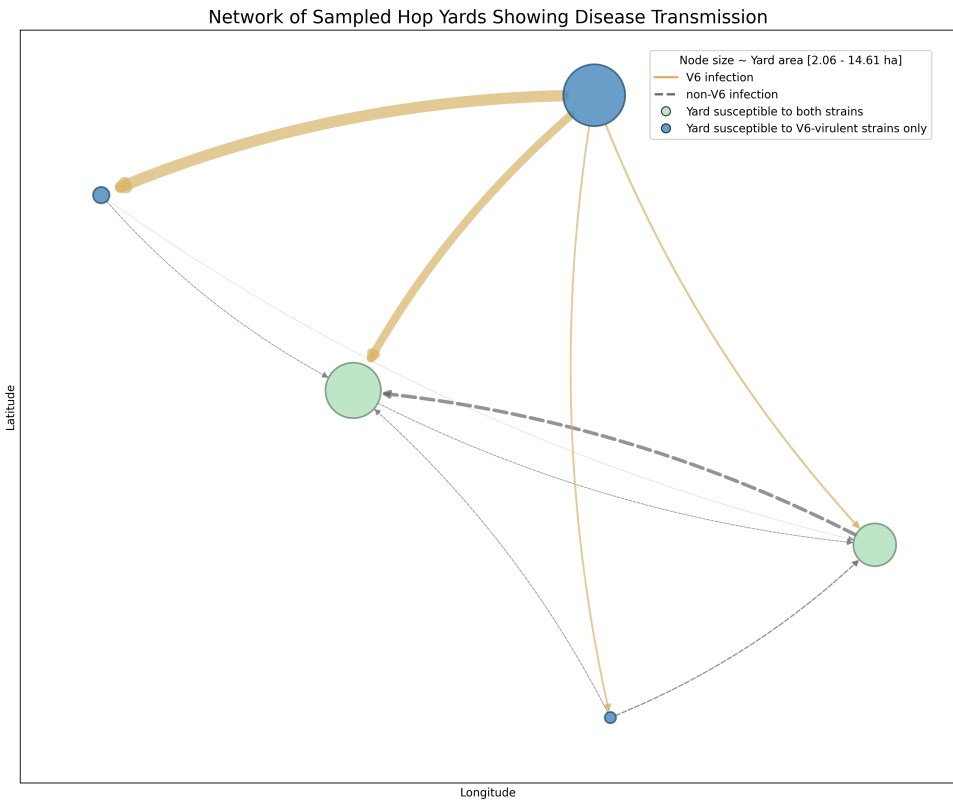


Figure 3: **Network of sampled hop yards by centrality quantiles.** This network visualization shows a representative sample of hop yards (one per centrality quantile) connected by inferred disease transmission pathways. Node sizes are proportional to yard area, with colors indicating disease status ( $tI=0$  in green,  $tI=1$  in blue). Edge colors and styles represent the source infection status ( $sI=1$  as solid brown lines,  $sI=0$  as dashed gray lines), with edge widths proportional to directed transmission weights based on area, wind patterns, and distance. The network illustrates the spatial structure of disease transmission potential across the production landscape.

this model by introducing two parameters that moderate disease in a given hop yard and disease spread from other hop yards based on the number of fungicide applications made in the prior month. We also generalized the model by expressing the dispersal kernel as a function of distance and source strength to accommodate various functional forms. The impact of exogenous inoculum depends jointly on the pathogen virulence in the source yards and susceptibility of the cultivar planted in the target yard.

The number of diseased plants is given by  $Y_i$ , among a sample of  $n_i$  plants, with  $i = 1, \dots, N$  indexing yard identity. The probability of  $Y_i$ , is taken as binomially distributed with the predictor function expressed on the log-odds scale as:

$$\log \left( \frac{p_i}{1 - p_i} \right) = \beta + \delta \left( \frac{\tilde{y}_i}{n_{\tilde{y}_i}} \exp(-\eta_1 s_i) \right) + \gamma \sum_{j=1}^{M_i} \left( \frac{a_j z_j}{n_{z_j}} w_{ij} \exp(-\eta_2 s_j) f(d_{ij}; \alpha) \right) \quad (1)$$

Covariates and parameter interpretations are given in Tables 1 and 2. Parameters are allowed to vary for time transition periods from May to June and from June to

July. The equation defines the model for disease development on foliage at the plant [272](#) scale. We explored an exponential and also a power-law function for the dispersal kernel, [273](#) but present results only for the power-law function, given theoretical considerations of [274](#) expected dispersal characteristics of *P. macularis*. [275](#)

Table 1: Covariate notations for each yard of interest  $i = 1, \dots, N$  in a particular month, and all other yards  $j = 1, \dots, M_i$  relative to yard  $i$ .

Variable	Description
$\tilde{y}_i$	Number of diseased plants at yard $i$ in the prior month
$n_{\tilde{y}_i}$	Number of plants sampled at yard $i$ in the prior month
$a_i$	Area (hectares) of yard $i$
$z_j$	Number of diseased plants at yard $j$ in the prior month
$n_{z_j}$	Number of plants sampled at yard $j$ in the prior month
$a_j$	Area (hectares) of yard $j$
$d_{ij}$	Distance (kilometers) from centroids of yard $i$ to yard $j$
$w_{ij}$	Wind vector on $j - i$ direction in the prior month
$s_i$	Number of fungicide sprays in yard $i$ in prior month
$s_j$	Number of fungicide sprays in yard $j$ in prior month

Table 2: Interpretation of model parameters.

Parameter	Interpretation
$\beta$	Baseline log-odds of disease, after accounting for autoinfection and dispersal.
$\delta$	Change in log-odds of disease associated with autoinfection at the yard scale, after accounting for disease spread.
$\gamma$	Distance-adjusted change in log-odds of disease associated with disease spread from other yards, after accounting for autoinfection.
$\alpha$	Dispersal parameter providing distance adjustment to change in log-odds of disease associated with individual source yards.
$\eta_1$	Change in log-odds of disease associated with autoinfection at the yard scale, after accounting for fungicide sprays.
$\eta_2$	Dispersal parameter providing fungicide spray adjustment to change in log-odds of disease associated with individual source yards.

### 2.5.2 Economic model

[276](#)

The profit function  $\Pi$  at time  $t$  over the growing season ( $t = 0, \dots, T$ ) measures the total [277](#) profit per hectare across all hop yards  $i = 1 \dots N$ . [278](#)

$$\Pi(s_{it}) = \sum_{i=1}^N (\pi_{it})$$

where  $\pi_{it}$  is the profit per hectare at time  $t$  for yard  $i$ . This profit equation is conditioned on the number of fungicide sprays  $s_{it}$  across the season and subject to constraints [279](#) [280](#)

imposed by the epidemic network model and by the price-quality relationships detailed 281  
below. Here, we assume risk neutrality of growers. 282

The profit  $\pi_{it}$  for each yard  $i$  at time  $t$  is defined as the difference between revenue 283  
and cost for each yard at time  $t$ : 284

$$\pi_{it} = R_t(q_i, v; p_i) - C_i(s_{it})$$

Revenue is only realized in the final period  $T$ , so that revenue is defined by  $R_i(q_i, v; p_i) = 285$   
 $R_T$ , otherwise  $R_i(q_i, v; p_i) = 0$ . Revenue is a function of both yield  $q_i$  and price  $v$ , condi- 286  
tioned on the disease probability level  $p_i$ . Costs  $C_i$ , defined in more detail below, are a 287  
function of fixed costs and the number of fungicide sprays,  $s_{it}$ . 288

Both yield quantity and price are adjusted by the incidence of cones with disease and 289  
associated quality defects as inferred from cone color. We used relationships reported in 290  
the literature to link the foliar phase of the disease to incidence of cones with powdery 291  
mildew, yield, and defects to cone color. First, the incidence of leaves with powdery 292  
mildew was estimated from the incidence of plants,  $p_i$ , with powdery mildew through the 293  
hierarchical relationship between disease at these scales: 294

$$\text{Leaf Incidence} = 1 - (1 - p_i)^{D/n}$$

where  $n$  is the number of leaves sampled per plant and  $D$  is the index of dispersion. 295  
We assume  $n = 50$  and  $D$  as reported previously. The incidence of cones with powdery 296  
mildew was assumed to be a linear function of the incidence of leaves with powdery mildew 297  
as: 298

$$\text{Cone Incidence} = a_1 \times \text{Leaf Incidence} + b_1$$

Yield loss was then estimated assuming a linear relationship with cone incidence, which 299  
is in turn derived from leaf incidence: 300

$$\text{Yield Loss} = a_2 \times \text{Cone Incidence}$$

We considered cone color a surrogate for quality defects associated with powdery 301  
mildew that could lead to crop devaluation or rejection based on production contract 302  
standards. Cone color was modeled using an industry-accepted 10-point scale (Lafontaine 303  
& Shellhammer, 2015) as an exponential decay function: 304

$$\text{Cone Color} = 10 + a_3 \cdot (1 - \exp(-b_3 \times \text{Cone Incidence}))$$

These empirical relationships are presented in Figure 5. 305

Market conditions and production contracts also impact revenue as shown in Figure 306  
4. Production contracts were reviewed and plausible damage functions were derived from 307  
expert opinion for crop devaluation from moderate damage, salvage value if the crop 308

was severely affected and was alternatively extracted for alpha-acids, or unsaleable due 309  
to extreme damage. We modeled these scenarios as a sigmoid function with varying 310  
thresholds dependent on low, medium, and high market demand, as: 311

$$\text{Adjusted Price} = \text{Initial Price} \times \sigma(\theta_0 + \theta_1 \cdot \text{Cone Color})$$

where  $\sigma$  is the sigmoid function and  $\theta_0, \theta_1$  are parameters estimated for different 312  
market demand scenarios. Revenue in a given yard is then calculated as the product 313  
of Adjusted Price and expected yield. Yield in the absence of disease was taken as the 314  
average yield reported in 2020 by the National Agricultural Statistics Service for the 315  
four cultivars we considered, as we describe below. The initial price was taken from 316  
representative production contracts for each of the three estimated levels of demand. 317

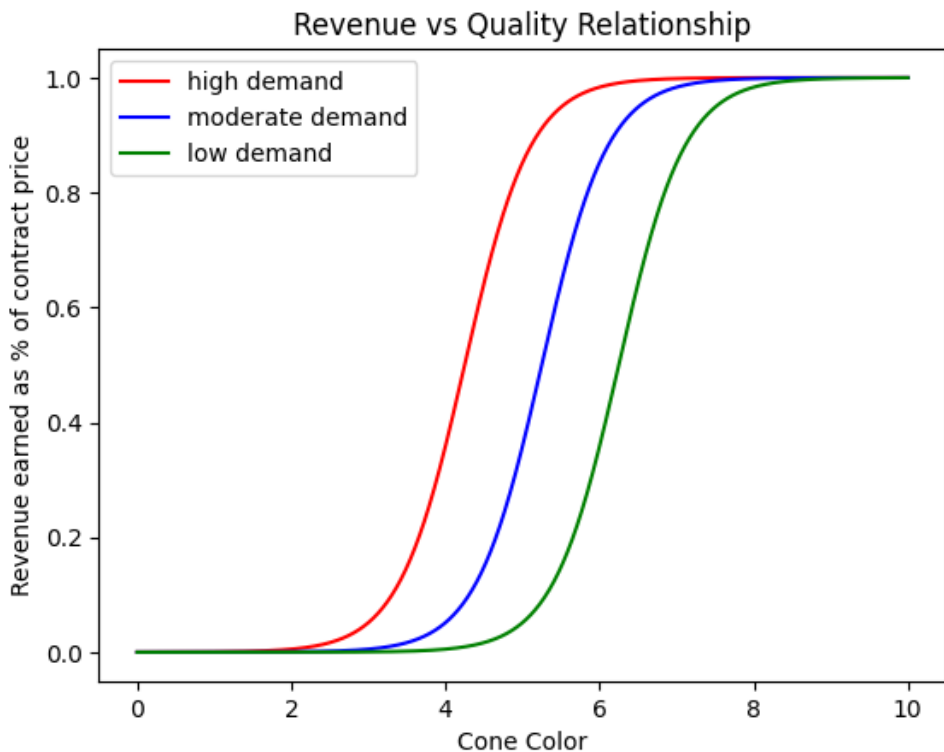


**Figure 4: Relationship between crop quality and revenue under different market demand scenarios.** Sigmoid functions model the relationship between hop cone quality (measured by cone color on a 10-point scale) and the revenue earned as a percentage of the contract price. The curves illustrate three distinct market demand scenarios: high, moderate, and low. Under low demand (green curve), stricter quality standards are enforced, meaning a higher cone color score is required to achieve the full contract price compared to moderate (blue curve) or high (red curve) demand conditions. These functions are used in the economic model to calculate crop devaluation based on simulated disease levels.

The cost function for each hop yard  $C_i$  incorporates the costs associated with fungicide 318  
sprays along with fixed costs and other variable costs over the production season: 319

$$C_i(s_{i,t}) = C_F + C_V + \sum_{t=0}^T (C_{s,t} + C_{a,t})$$

where  $C_F$  is the fixed cost,  $C_V$  represents other variable costs,  $C_{s,t}$  is the fungicide cost, and  $C_{a,t}$  is the application cost at period  $t$ . Fixed and other variable costs were obtained from Galinato (Galinato, 2020). 320  
321  
322

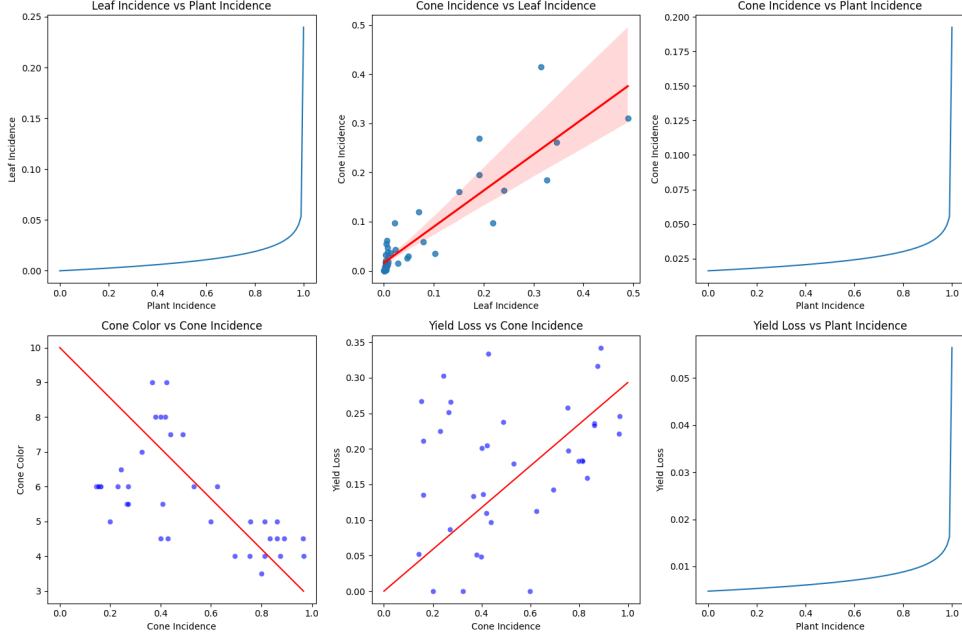


**Figure 5: Empirical relationships between disease incidence and crop damage.** Six panels show the fitted relationships used in the economic model: (A) Leaf incidence as a function of plant incidence, (B) Cone incidence versus leaf incidence with linear regression, (C) Cone incidence versus plant incidence, (D) Cone color degradation as a function of cone incidence, (E) Yield loss versus cone incidence with linear relationship, and (F) Yield loss versus plant incidence. These empirical relationships link the epidemiological model outputs to economic damage estimates for yield quantity and quality metrics. 323

### 2.5.3 Parameter estimation

The parameters in the epidemic network model were estimated using maximum likelihood. 324  
 The likelihood function was constructed by assuming the number of diseased plants  $Y_i$  in each yard  $i$  follows a binomial distribution with probability  $p_i$  given by the inverse logit of  $\eta_i$  in the equation above. The log-likelihood of the parameters  $\boldsymbol{\theta} = (\beta, \delta, \gamma, \alpha, \eta_1, \eta_2)$  325  
326  
327  
 given the observed data  $\mathcal{D} = (y_i, n_i, \tilde{y}_i, n_{\tilde{y}_i}, a_i, s_i, z_j, n_{z_j}, a_j, d_{ij}, w_{ij}, s_j)$  where  $i = 1 \dots N$  328  
 and  $j = 1 \dots M_i$  is: 329

$$\ell(\boldsymbol{\theta}; \mathcal{D}) = \sum_{i=1}^N [y_i \log p_i + (n_i - y_i) \log(1 - p_i)]$$

where  $p_i = \text{logit}^{-1}(\eta_i)$  and  $\eta_i$  is a function of  $\boldsymbol{\theta}$  and the observed covariates. 330

The maximum likelihood estimator  $\hat{\boldsymbol{\theta}}$  was obtained by maximizing  $\ell(\boldsymbol{\theta}; \mathcal{D})$  subject 331

to bounds on the parameters to ensure they were biologically plausible. This was done 332  
using the Sequential Least Squares Programming (SLSQP) algorithm, a gradient-based 333  
nonlinear constrained optimization method. Analytical expressions for the gradient and 334  
Hessian of the negative log-likelihood were derived and provided to the algorithm to 335  
improve convergence. Multiple random initializations of the parameters were used to 336  
ensure a global optimum was reached. The model was fit using data for all years, but 337  
separately for the May to June and June to July transition periods to allow parameters 338  
to vary between these periods. Convergence was assessed by monitoring the magnitude 339  
of the largest gradient and the positive definiteness of the Hessian matrix at the obtained 340  
solution. 341

All analyses were conducted in Python, making use of the NumPy, SciPy, and Stats- 342  
models libraries for numerical computing and statistical modeling. 343

### 3. Simulation experiments

For the simulation experiments described below, we constructed a synthetic landscape 345  
using the actual locations and sizes of hop yards in each of the years 2014 to 2017 from 346  
our data set. Each hop yard was planted to one of four representative cultivars (Chinook, 347  
Simcoe®, Nugget, or Mosaic®), chosen because they were commercially relevant at the 348  
time of this research, either possessed or did not possess the R6 resistance, and can be 349  
sold for direct use in brewing or alternatively can be processed to extract alpha-acids as a 350  
secondary market. We assumed equal susceptibility to powdery mildew given a compatible 351  
strain of pathogen. Cultivar assignments were made at random for each yard, subject to 352  
an approximately 1:1 ratio of cultivars that possess R6 or non-R6 in each of the quantiles 353  
as we describe below. The same yard-level assignments were used across simulation runs 354  
for a given year. 355

We initiated epidemics at the start of May under varying scenarios by specifying an 356  
initial probability of disease, which governed the expected frequency of initial infections 357  
(flag shoots) in the population of hop yards. In reality, any given yard may or may 358  
not harbor flag shoots, making the true distribution of early-season disease unknown. 359  
We therefore modeled the occurrence of initial infections stochastically as follows. For 360  
each yard in the landscape, we first identified the proportion of plants there that were 361  
susceptible, which depends on whether a yard was planted with a cultivar susceptible 362  
to V6-virulent and/or non-V6-virulent strains. We also identified which quantile of the 363  
degree-centrality distribution the yard occupied, where degree-centrality weights each yard 364  
by the product of yard area, average wind run, and a decreasing function of inter-yard 365  
distance as a measure of disease transmission potential. Denote this quantile by  $q_i$  for 366  
yard  $i$ , and let  $0 \leq q_i \leq 1$  (discretized into 20% quantile bins). 367

Next, we specified a desired mean initial probability of disease across the entire land- 368  
scape, denoted by  $p_0$ . Because yards differ in their centrality and susceptibility to a given 369

strain of the pathogen, we introduced an adjustment factor so that the final landscape-wide fraction of plants with flag shoots would closely match  $p_0$ . Specifically, within each centrality quantile  $q$ , let:

$$(\text{proportion susceptible in quantile } q) = \mathcal{S}_q, \quad (\text{proportion of yards in quantile } q) = \mathcal{P}_q.$$

We then scaled  $p_0$  by  $\frac{1}{\mathcal{S}_q} \frac{1}{\mathcal{P}_q}$ , effectively concentrating flag shoots into those yards that were actually susceptible in the particular quantile  $q$ . Denote this adjusted probability by  $p_0^*(q)$ . For each yard  $i$  in quantile  $q$ , we then drew:

$$y_{0,i} = \text{Binomial}(n_i, p_0^*(q)),$$

where  $n_i$  is the number of plants in yard  $i$ . Thus,  $y_{0,i}$  is the number of initial infections (flag shoots) in yard  $i$  at the start of May.  $y_{0,i}$  was set to zero if the initial strain that was randomly placed was biologically impossible with the cultivar in that yard.

With these initial conditions set, we simulated disease progression through May, June, July, and into the early cone-development period using the network-based epidemiological model described in Section 2. In each monthly step, the incidence of infected plants in yard  $i$  was predicted using the fitted coefficients from the equation above. Fungicide applications served as an input to the model via coefficients that reduce the rate of new infections in both the focal yard and the potential source yards; the number of sprays in a yard was itself predicted by a Poisson regression fitted from the data on how many fungicide applications growers made in a yard in response to the incidence of diseased plants in the previous month. In May, we specified that if a yard *did not* contain disease then it still received a baseline of 0.43 fungicide applications, which was the average number of sprays for yards with no disease in the raw data. We additionally allowed a user-defined number of early sprays in May for yards that *did* harbor at least one flag shoot (i.e.  $y_{0,i} > 0$ ). These early sprays could range from zero, no additional sprays beyond the baseline, up to 10 sprays to represent an extremely aggressive early-season spray strategy.

After simulating disease progress through the end of July, we computed the incidence of diseased cones using the relationship in Figure 1C. The economic model then used these incidence levels to estimate yield losses, potential quality reductions (via the cone-color model), and resulting net returns after accounting for fixed costs, variable costs, and the cost of sprays. We repeated these simulations for a range of  $p_0$  values, different fractions of V6-virulent strains present in the initial inoculum, and different yard-level centralities in which the initial flag shoots occurred. For the primary inoculum dose, we varied  $p_0$  from  $10^{-5}$  to  $10^{-2}$ , a large but plausible range of primary infection levels. The proportion of initial infections caused by V6 or non-V6-virulent strains was varied from 0% to 100% in 25% steps. For degree centrality, we placed the primary inoculum into

each 20% quantile. Unless otherwise noted, each scenario was run 100 times to capture 404 variability in binomial draws. We report either the mean or percentiles of the *relative* 405 change in profit per hectare compared to a no-disease/no-spray baseline. 406

### 3.1 Summary of simulation parameters

407

Table 3: Key parameters varied in the simulation, their tested ranges, and the rationale or source.

Parameter	Values Tested	Rationale / Data Source
Year	2014, 2015, 2016, 2017	Real yard size, distance, and wind patterns were available for each year, reflecting distinct conditions.
Simulations	100	Each scenario is replicated to capture variability from binomial draws of initial disease.
Quantiles	5	Yards are classified into five bins by degree-centrality, used when varying location-based initial infections.
Pathogen- diversity	0.0, 0.25, 0.50, 0.75, 1.0	Varies fraction of initial inoculum from V6-virulent vs. non-V6-virulent strains.
Sprays in May	0, 1, 2, 3, 4, 5, 6, 7, 8, 9, 10	Extra sprays (beyond baseline) if a yard has flag shoots. Upper end (10) tests diminishing returns.
Initial infection probability ( $p_0$ )	$10^{-5}, 5 \times$ $10^{-5}, 10^{-4}, 5 \times$ $10^{-4}, 10^{-3}, 5 \times$ $10^{-3}, 10^{-2}$	Represents the probability of a plant harboring an overwintered infection. Spans extremely rare ( $10^{-5}$ ) to moderately frequent ( $10^{-2}$ ).
Market scenario	low, moderate, high	Captures three contrasting demand/price structures, impacting crop value and quality penalties.

Beyond these parameters, the simulation code uses yard-level attributes (area, distance 408 matrices, wind data) and the fitted model coefficients described in Sections 2 and 3. In 409 each scenario, the model outputs include time series of disease incidence and final net 410 profit estimates under the specified market-demand conditions. 411

## 4. Results

412

### 4.1 Parameter estimates for epidemic model

413

To understand the temporal dynamics of the epidemic model, we compared the parameter 414 estimates for the two key transition periods: May-June and June-July (Table 4). Several 415 notable differences emerge between these periods. 416

Table 4: Parameter estimates for epidemic model

Parameter		May–June	June–July
<b>Epidemic Model</b>			
$\beta_1$	Baseline log-odds	-2.06	-2.79
$\beta_2$	Baseline log-odds	-4.15	-3.88
$\delta_1$	Autoinfection effect	2074.35	2.94
$\delta_2$	Autoinfection effect	120.46	8.04
$\gamma_1$	Dispersal effect	34358.91	1390.71
$\gamma_2$	Dispersal effect	14536.03	286.8
$\alpha_1$	Dispersal kernel	0.71	1.0
$\alpha_2$	Dispersal kernel	2.67	2.04
$\eta_{11}$	Fungicide effect	3.51	0.02
$\eta_{12}$	Fungicide effect	1.62	0.31
$\eta_{21}$	Fungicide effect	2.9	0.95
$\eta_{22}$	Fungicide effect	0.27	0.37

The baseline log-odds of disease ( $\beta_1, \beta_2$ ) were lower (more negative) in May–June (- 417  
2.06, -4.15) than in June–July (-2.79, -3.88), indicating a lower baseline risk of disease 418  
early in the season. The effect of autoinfection ( $\delta_1, \delta_2$ ) was much larger in May–June 419  
(2074.35, 120.46) compared to June–July (2.94, 8.04), suggesting that local sources of 420  
inoculum are most influential at the start of the epidemic. The effect of dispersal from 421  
other yards ( $\gamma_1, \gamma_2$ ) was also much greater in May–June (34358.91, 14536.03) than in 422  
June–July (1390.71, 286.8), highlighting the importance of regional spread early in the 423  
epidemic. The dispersal kernel parameters ( $\alpha_1, \alpha_2$ ) were larger in June–July (1.0, 2.04) 424  
than in May–June (0.71, 2.67), indicating a possible shift in the spatial scale of dispersal 425  
as the season progresses. The fungicide effect parameters ( $\eta_{11}, \eta_{12}, \eta_{21}, \eta_{22}$ ) were generally 426  
larger in May–June, especially  $\eta_{11}$  (3.51 vs 0.02), suggesting that fungicide applications 427  
are more impactful on reducing disease early in the season versus later. Overall, these 428  
differences indicate that both local and regional sources of inoculum are most important 429  
in the early epidemic phase, and that fungicide applications have their greatest impact 430  
when applied earlier in the epidemic. As the season progresses, the epidemic becomes less 431  
sensitive to these factors. 432

## 4.2 Simulation experiments

The simulation results demonstrate a strong dependence of profitability on initial epidemic 434  
conditions, specifically highlighting the influence of initial inoculum dose, pathogen di- 435  
versity, and the dispersal centrality of the initially infected yards on disease management 436  
strategies (Figure 6). We address each of these points in the sections that follow. 437

### 4.2.1 Impact of initial inoculum dose

The initial probability of disease ( $p_0$ ) emerged as a dominant factor influencing the prof- 439  
itability and efficacy of fungicide applications (Figure 6). 440

**Low Inoculum** ( $p_0 \leq 10^{-4}$ ): Across all market demand scenarios, when the initial probability of disease was very low ( $p_0 = 10^{-5}$  or  $5 \times 10^{-5}$ ), the relative change in profit remained close to zero regardless of the number of fungicide sprays in May. For example, in 2014 under low demand, the profit change was consistently between 0% and -1% for all spray numbers and degree-centrality percentiles.

**Moderate to High Inoculum** ( $p_0 \geq 10^{-3}$ ): As  $p_0$  increased, profitability became more sensitive to the number of sprays. For  $p_0 = 5 \times 10^{-3}$  or  $10^{-2}$ , failing to spray (0 sprays) resulted in profit losses of up to -10%. Profit loss was most severe in high centrality yards and under high market demand.

In contrast, applying 4-6 sprays in May minimized losses, with profit changes typically between -1% and -3%. For example, in the high-demand scenario, at  $p_0 = 10^{-2}$ , 0 sprays led to losses of -10% to -12% in the most central yards, while 5-6 sprays reduced losses to about -2% to -3%.

#### 4.2.2 Effect of pathogen diversity

Pathogen strain diversity also played an influential role, particularly in scenarios where the pathogen population included varying proportions of the V6-virulent strain capable of infecting a broader range of cultivars. As the proportion of the V6-virulent strain increased, the optimal number of fungicide sprays required to maximize profitability rose accordingly. When pathogen populations consisted predominantly or entirely of the V6-virulent strain, fungicide applications became increasingly essential to maintaining profitability. Thus, pathogen diversity directly affected both the necessity and frequency of fungicide interventions.

Quantitatively, in the high-demand scenario for  $p_0 = 10^{-2}$  and 100% V6, profit losses without spraying reached -10% to -12%, whereas 5-6 sprays reduced losses to -2% to -3%.

#### 4.2.3 Influence of degree-centrality of initial inoculum

The location of initial infections, as measured by the degree-centrality of initially infected yards, significantly impacted profitability, particularly under high inoculum pressure scenarios. Initial infections in highly central yards were more detrimental, exacerbating the spread and subsequent economic losses across the region. For example, in the high-demand scenario at  $p_0 = 10^{-2}$ , 0 sprays led to losses of -10% to -12% in the most central yards, compared to -6% to -8% in the least central yards. In contrast, when initial infections occurred in less central yards, the relative economic losses were reduced, particularly under higher market demand scenarios.

#### 4.2.4 Market demand conditions

Different market demand conditions notably influenced the optimal disease management strategy. Under high market demand conditions, the impact of early fungicide interventions on profitability was moderate, reflecting more flexible quality standards. Conversely,

under moderate and low market demand conditions, where quality requirements were more 478  
stringent, profitability was much more sensitive to fungicide application strategies. In- 479  
creased fungicide use was essential under these lower demand scenarios to prevent severe 480  
quality-related profit reductions. For instance, under low demand, the economic penalty 481  
for under-spraying was greatest, with losses up to -10% at high  $p_0$  and 0 sprays, and only 482  
reduced to -2% to -3% with 5-6 sprays. These patterns were consistent across all four 483  
years of the study period (Figures 8, 9, and 10). 484

## 5. Discussion 485

Our analysis addresses a multifaceted challenge in agricultural disease management where 486  
epidemic control decisions must account for complex interactions between pathogen bio- 487  
logy, management practices, market conditions, and regional-scale disease transmission. 488  
Our motivating pathosystem represents a complex scenario for economic epidemiology, 489  
combining the spread of a highly dispersible pathogen capable of long-distance trans- 490  
mission, potential damage to both yield and quality metrics, market-sensitive quality 491  
standards, and strain-specific cultivar resistance, creating a heterogeneous landscape of 492  
host connectivity. This complexity necessitates a modeling approach that simultaneously 493  
captures network-scale disease transmission, multi-dimensional crop damage functions, 494  
and market-dependent economic outcomes. Three key findings emerge from our simula- 495  
tions. First, epidemic control is exquisitely sensitive to conditions in the earliest stages 496  
of outbreaks, with relatively small changes in initial inoculum dose and early-season fun- 497  
gicide applications translating to substantial economic differences. Second, there appears 498  
to exist a critical threshold in pathogen pressure below which intensive management be- 499  
comes unnecessary, suggesting opportunities for area-wide interventions targeting primary 500  
inoculum reduction. Third, quality-sensitive market conditions paradoxically drive more 501  
intensive fungicide use under depressed demand scenarios, challenging traditional eco- 502  
nomic injury level concepts when crop value is tied to quality standards rather than yield 503  
alone. 504

### 5.1 Early intervention and threshold effects 505

One of the most striking findings from our simulations is the threshold-like response in 506  
simulated optimal control strategies as initial inoculum probability increases. When the 507  
initial probability of disease remained below  $10^{-4}$ , economic losses were minimal regardless 508  
of fungicide application intensity, pathogen strain diversity, or initial infection location. 509  
Above this threshold, however, the system exhibited dramatic sensitivity to early-season 510  
intervention, with the optimal number of fungicide applications in the first month be- 511  
coming the dominant factor determining economic outcomes. This pattern aligns with 512  
theoretical predictions for epidemics where containment efficiency depends critically on 513  
early-stage contact rates and intervention timing (Margosian et al., 2009; Severns et al., 514

2019). For spatially-explicit epidemics with long-distance dispersal capabilities, small 515 changes in primary inoculum can cascade through the transmission network, leading to 516 nonlinear responses in final epidemic size (Cunniffe, Koskella et al., 2015). Epidemic 517 threshold behavior has been documented across diverse host-pathogen systems, from live- 518 stock diseases (Hartfield & Alizon, 2013) to forest pathogens (Lofgren et al., 2014). Similarly, 519 the sensitivity to early intervention aligns with the "golden hour" concept in human 520 disease outbreak response, where rapid action in the initial stages determines overall out- 521 break severity (Fraser et al., 2004). In most susceptible-infected-recovered (SIR) epidemic 522 models, there is a critical value of R below which epidemics cannot occur (Diekmann et 523 al., 2013; Keeling & Eames, 2005). The critical value of R depends on transmission and 524 recovery dynamics, but also the structure of the host population and mixing of healthy 525 and infected individuals. Calculation of a threshold R becomes increasingly difficult with 526 more complex epidemic models. Thresholds occur not only for epidemic development, but 527 also for management intervention in social dilemma problems, such as collective action 528 in the form of area-wide pest management (Cunniffe & Gilligan, 2024; Lence & Singer- 529 man, 2022). Identifying participation thresholds in complex social-ecological systems is 530 not trivial, and often participation thresholds for successful area-wide pest management 531 are unknown due to uncertainty on factors such as transmission dynamics of the patho- 532 gen or vector, heterogeneity in host connectivity, and efficacy of the intervention effort 533 at different scales (Cunniffe & Gilligan, 2024). Our simulation experiments with a time- 534 transition epidemic model suggest that there exists a primary inoculum threshold effect 535 in the motivating pathosystem and, very likely, other pathosystems where epidemics are 536 the result of inoculum and intervention efforts that influence disease spread both within 537 and among management units. We expect that the observed initial inoculum threshold 538 results from the specific combination of pathogen transmission and landscape connectivity 539 idiosyncratic to the specific conditions in the motivating pathosystem. How these specific 540 factors influence the dynamics of landscape-level epidemics is an obvious area for future 541 investigation. 542

Our study indicates that epidemic mitigation may not require intensive early-season 543 intervention when the primary inoculum at the landscape level is sufficiently low. Indeed, 544 we observed that a 10-fold reduction in initial inoculum from the levels observed in prac- 545 tice (Gent et al., 2018) could largely eliminate economic damage from powdery mildew 546 industry-wide. Further work is needed to understand whether area-wide interventions tar- 547 geting primary inoculum reduction may be more cost-effective than field-level fungicide 548 intensification. This might involve strategic deployment of cultural control measures or 549 host resistance that is race-nonspecific. 550

When the primary inoculum dose is not limiting, we show it is possible to calibrate 551 intervention efforts to observed or expected primary inoculum dose and location. More 552 intensive early-season intervention is warranted when primary inoculum occurs in indi- 553 vidual fields that are more highly connected in the disease transmission network or when 554

the initial infections are caused by virulent strains that can infect more cultivars. The importance of intervention in highly connected nodes is well established in network epidemiology across physical and biological systems (Cross et al., 2004; Pastor-Satorras & Vespignani, 2001). Minimizing economic loss was sensitive to the number of fungicide applications made in the earliest stage of epidemics, and this was particularly the case when primary inoculum first occurred in the most highly connected yards. In our analysis, under severe epidemic conditions ( $p_0 = 10^{-2}$  and 100% V6 strain under high market demand), achieving a similar economic outcome required four more fungicide applications in the first month of epidemics when primary inoculum was concentrated in the most connected yards versus the least connected in the network. We observed similar changes in the optimal simulated number of fungicide applications when the pathogen population increased from a single, less virulent strain to entirely a more virulent strain that could infect all cultivars. Degree centrality is calculated from yard size, distance to other yards, and average wind run, features that are known or can be estimated prior to epidemic development. In some instances, pathogen virulence may be known with certainty depending on which cultivar develops disease (Gent et al., 2019). Given this, one may estimate the management units that we predict are most critical for disease spread and therefore prioritize intensified management efforts prior to or in the earliest stages of a disease outbreak.

## 5.2 Market sensitivity and economic injury level paradigms

The optimal spray strategy remained largely consistent across different market demand scenarios, typically realizing 4-6 applications for interventions during the critical early epidemic period when primary inoculum pressure was substantial. The simulated optimum number of sprays was slightly higher under high market demand conditions but decreased modestly under moderate and low demand scenarios, with low demand scenarios realizing a decrease by an average of 1 spray. Across the market demand scenarios, the highest profits were consistently associated with overtreatment rather than undertreatment. This asymmetry in marginal profit loss has important implications for understanding the economic consequences of suboptimal spray decisions. While overtreatment of fungicide applications led to diminishing returns and net economic losses through higher input costs, these losses from overtreatment were lesser in magnitude than the losses incurred from a modest undertreatment relative to the simulated optimum.

It is important to note that incorporating uncertainty or risk aversion into the profit maximizing decision process predicts increased applications of pesticides relative to a risk neutral grower (Feder, 1979). Furthermore, more stringent quality standards and increased uncertainty of the likelihood of pathogens also tend to increase pesticide use in crop production (Marsh et al., 2000).

This pattern reflects a broader challenge in crops where farm profit depends on meeting specific quality criteria in contracts rather than simply maximizing yield. When crop rejec-

tion or severe devaluation becomes possible, risk-averse growers may adopt more intensive 594 management strategies that exceed the classical EIL optimization (Feder, 1979). Under 595 high pathogen pressure in our simulations, the economic penalty for under-treatment be- 596 came as severe as over-treating by two to three times the simulated optimal level. The 597 sensitivity of private optimal strategies to market conditions has important implications 598 for pest management recommendations and policy. Management recommendations are 599 often targeted based on disease pressure and tacitly assume static market demand. Our 600 results suggest that market context should also inform management decisions (Marsh et 601 al., 2000). Furthermore, vague terms in production contracts regarding quality standards 602 or price premiums may exacerbate this issue by increasing uncertainty and encouraging 603 more conservative (intensive) disease intervention. 604

### 5.3 Study limitations and future directions 605

Several limitations should be considered when interpreting our results. We recognized 606 that the damage functions linking disease incidence to cone color and subsequent price 607 adjustments rely on relationships derived from literature rather than direct observation. 608 This may introduce uncertainty in the precise magnitude of the economic effects we es- 609 timate in the damage functions. However, the directional and relative importance of 610 the epidemic factors and management interventions we report remain valid. Ambiguous 611 language in production contracts is problematic and also complicates model parameter- 612 ization, but there are no easy solutions to this problem. Indeed, this may be the largest 613 source of uncertainty in our modeling and also one of the most difficult to model precisely. 614

We focused on annual profit maximization at the landscape-level as our outcome of 615 interest. This may be appropriate for producers with productivist ideology (McDowell 616 et al., 2018) but ignores grower risk aversion and externalities whose costs are not 617 borne directly by producers. We also do not identify the optimal strategy for an indi- 618 vidual grower or an individual yard. Many other production or environmental objectives 619 could be considered, and at time steps longer than a single crop year. Nonetheless, the 620 coupled epidemiological-economic modeling framework we developed provides a founda- 621 tion for analyzing other production objections or interventions in complex pathosystems 622 and production scenarios. 623

## 6. Appendix 624

We expand on the generalized regression model developed in previous work. For a given 625 yard  $i$ , we estimate the log-odds of disease  $\eta_i$  given by 626

$$\eta_{i,\tau} = \sum_{k=1}^K I_k^{(t)}(i) \left[ \beta_{k,\tau} + \delta_{k,\tau} \left( \frac{\tilde{y}_i}{n_{\tilde{y}_i}} \exp(-\eta_{1k}s_i) \right) + \gamma_{k,\tau} \sum_{j=1}^{M_i} \left( \frac{a_j z_j}{n_{z_j}} \exp(-\eta_{2k}s_j) w_{ij} \exp(-\alpha_{k,\tau}d_{ij}) I_k^{(s)}(j) \right) \right]$$

## 6.1 Parameter estimates

627

Table 5: Parameter estimates for epidemic model

Parameter	May–June	June–July
<b>Epidemic Model</b>		
$\beta_1$	Baseline log-odds	−2.06
$\beta_2$	Baseline log-odds	−4.15
$\delta_1$	Autoinfection effect	2074.35
$\delta_2$	Autoinfection effect	120.46
$\gamma_1$	Dispersal effect	34358.91
$\gamma_2$	Dispersal effect	14536.03
$\alpha_1$	Dispersal kernel	0.71
$\alpha_2$	Dispersal kernel	2.67
$\eta_{11}$	Fungicide effect	3.51
$\eta_{12}$	Fungicide effect	1.62
$\eta_{21}$	Fungicide effect	2.9
$\eta_{22}$	Fungicide effect	0.27
		0.37

Table 6: Parameter estimates for damage functions

Parameter	Estimate
<b>Cone Incidence Model</b>	
$a_1$	0.234
$b_1$	1.456
<b>Yield Loss Model</b>	
$a_2$	0.178
<b>Cone Color Model</b>	
$a_3$	0.312
$b_3$	2.147
<b>Adjusted Price Model (Sigmoid Function)</b>	
<i>High Demand</i>	$\theta_0$
	18.50
	$\theta_1$
<i>Moderate Demand</i>	$\theta_0$
	14.75
	$\theta_1$
<i>Low Demand</i>	$\theta_0$
	11.00
	$\theta_1$
	0.35

## 6.2 Poisson Regression Model for Fungicide Applications

628

As referenced in the Simulation Experiments section, the number of fungicide applications 629 was not a fixed input but was instead dynamically predicted to simulate realistic grower 630 behavior in response to observed disease. We modeled the number of fungicide applica- 631 tions in a given period as a function of the observed disease incidence in the previous 632 period using data from our field surveys from 2014 to 2017. 633

Given that the number of sprays is non-negative integer count data, a Poisson regres- 634 sion model was selected as the appropriate statistical framework. The model assumes that 635

the number of sprays,  $S_t$ , in a given month  $t$  follows a Poisson distribution with a mean  $\lambda_t$  636 that depends on the mildew incidence,  $I_{t-1}$ , from the previous month. The relationship 637 is expressed via a log-linear link function: 638

$$\log(\lambda_t) = \beta_0 + \beta_1 I_{t-1}$$

In this formulation,  $\beta_0$  is the intercept, representing the baseline log-count of sprays 639 when disease incidence is zero. The coefficient  $\beta_1$  quantifies the change in the log-count of 640 sprays for each unit increase in mildew incidence in the preceding month. The expected 641 number of sprays can thus be calculated as  $\lambda_t = \exp(\beta_0 + \beta_1 I_{t-1})$ . 642

Using grower records of fungicide use and our monthly disease assessments, we fitted 643 three separate models to capture spraying decisions at different stages of the growing 644 season: 645

- **June Sprays:** The number of sprays in June was modeled as a function of the 646 mean mildew incidence observed in May. 647
- **July Sprays:** The number of sprays in July was modeled as a function of the mean 648 mildew incidence observed in June. 649
- **Late-Season Sprays:** The number of sprays applied after July (late season) was 650 modeled as a function of the mean mildew incidence observed in July. 651

Each model was fitted using the Generalized Linear Model (GLM) implementation in 652 the ‘statsmodels’ library in Python, specifying a Poisson family with a log link. These 653 empirically-derived models were then integrated into the main simulation framework. In 654 each time step of a simulation run, the disease incidence from the previous month was 655 used as a predictor to generate an expected number of fungicide applications for each 656 yard. This approach allowed us to endogenously determine management costs based on 657 the simulated severity of the epidemic, thereby linking disease progression directly to 658 economic outcomes. 659

### 6.3 Supplementary results 660

### 6.4 Sensitivity analysis 661

Additional sensitivity analyses were conducted to evaluate model robustness to parameter 662 uncertainty. Key findings include: 663

- Doubling fungicide costs reduced optimal application frequency by 1-2 applications 664 but did not eliminate the threshold behavior 665
- Increasing quality penalty rates by 50% intensified optimal management strategies, 666 particularly under low market demand 667

- Alternative transmission kernel parameterizations (exponential vs. power-law decay) had minimal impact on optimal strategies 668  
669
- Network structure sensitivity analysis using different distance thresholds confirmed the importance of highly connected nodes 670  
671

The robustness of the threshold behavior across parameter variations supports the generalizability of our findings to similar pathosystems with quality-sensitive markets and network-scale disease transmission. 672  
673  
674

## Acknowledgements

675

We thank the many individuals that provided technical support for this project and the participating grower cooperators that provide access to their fields and production records. This research was conducted in support of U.S. Department of Agriculture CRIS project 2072-21000-061-000-D. Funding was provided by National Institute of Food and Agriculture Specialty Crop Research Initiative award number (2021-51181-35901).

## References

681

- Bassanezi, R., Montesino, L., Gimenes-Fernandes, N., Yamamoto, P., Gottwald, T., Amorim 682  
L., & Filho, A. (2013). Efficacy of area-wide inoculum reduction and vector con- 683  
trol on temporal progress of huanglongbing in young sweet orange plantings. *Plant 684  
Disease*, 97, 789–796. <https://doi.org/10.1094/PDIS-03-12-0314-RE> 685

Cross, P., Lloyd-Smith, J., Bowers, J., Hay, C., Hofmeyr, M., & Getz, W. (2004). Integrat- 686  
ing association data and disease dynamics in a social ungulate: Bovine tuberculosis 687  
in African buffalo in the Kruger National Park. *Annales Zoologici Fennici*, 41, 879– 688  
892. 689

Cunniffe, N., & Gilligan, C. (2024). Optimizing and implementing area-wide integrated 690  
pest management to mitigate resistance evolution. *Annual Review of Phytopatho- 691  
logy*, 62, 117–140. <https://doi.org/10.1146/annurev-phyto-121423-041950> 692

Cunniffe, N., Koskella, B., Metcalf, C., Parnell, S., Gottwald, T., & Gilligan, C. (2015). 693  
Thirteen challenges in modelling plant diseases. *Epidemics*, 10, 6–10. [https://doi.org/10.1016/j.epidem.2014.06.002](https://doi. 694<br/>org/10.1016/j.epidem.2014.06.002) 695

Cunniffe, N., Stutt, R., DeSimone, R., Gottwald, T., & Gilligan, C. (2015). Optimising 696  
and communicating options for the control of invasive plant disease when there is 697  
epidemiological uncertainty. *PLoS Computational Biology*, 11(4), e1004211. [https://doi.org/10.1371/journal.pcbi.1004211](https: 698<br/>//doi.org/10.1371/journal.pcbi.1004211) 699

de Waard, M., Georgopoulos, S., Hollomon, D., Ishii, H., Leroux, P., Ragsdale, N., & 700  
Schwinn, F. (1993). Chemical control of plant diseases: Problems and prospects. 701  
*Annual Review of Phytopathology*, 31, 403–421. [https://doi.org/10.1146/annurev.py.31.090193.002155](https://doi.org/10.1146/annurev. 702<br/>py.31.090193.002155) 703

Diekmann, O., Heesterbeek, H., & Britton, T. (2013). *Mathematical tools for understand- 704  
ing infectious disease dynamics*. Princeton University Press. 705

Estep, L., Sackett, K., & Mundt, C. (2014). Influential disease foci in epidemics and un- 706  
derlying mechanisms: A field experiment and simulations. *Ecological Applications*, 707  
24, 1904–1914. <https://doi.org/10.1890/13-1408.1> 708

Feder, G. (1979). Pesticides, information, and pest management under uncertainty. *Amer- 709  
ican Journal of Agricultural Economics*, 61, 97–103. [https://doi.org/10.2307/1239498](https://doi.org/10.2307/ 710<br/>1239498) 711

- Filho, A., Inoue-Nagata, A., Bassanezi, R., Belasque, J., Amorim, L., Macedo, M., Barbosa, J., Willocquet, L., & Savary, S. (2016). The importance of primary inoculum and area-wide disease management to crop health and food security. *Food Security*, 8, 221–238. <https://doi.org/10.1007/s12571-015-0544-8>
- Fraser, C., Riley, S., Anderson, R., & Ferguson, N. (2004). Factors that make an infectious disease outbreak controllable. *Proceedings of the National Academy of Sciences*, 101, 6146–6151. <https://doi.org/10.1073/pnas.0307506101>
- Galinato, S. (2020). *2020 cost estimates of establishing and producing hops in the Pacific Northwest* (Technical Bulletin No. TB38E). Washington State University Extension.
- Gent, D., Barbour, J., Dreves, A., James, D., Parker, R., & Walsh, D. (2016). Field evaluation of hop powdery mildew management programs. *Plant Disease*, 100, 1153–1160. <https://doi.org/10.1094/PDIS-10-15-1232-RE>
- Gent, D., Claassen, B., Gadoury, D., Grünwald, N., Knaus, B., Radišek, S., Weldon, W., Smart, C., & Pfender, W. (2018). Population genetic structure of *podosphaera macularis* and implications for managing hop powdery mildew in the Pacific Northwestern United States. *Phytopathology*, 108, 1212–1222. <https://doi.org/10.1094/PHYTO-04-18-0127-R>
- Gent, D., Claassen, B., Twomey, M., Wolfenbarger, S., Woods, J., & Probst, C. (2019). Virulence and aggressiveness of *podosphaera macularis* on hop cultivars with different resistance genes. *Phytopathology*, 109, 1193–1204. <https://doi.org/10.1094/PHYTO-12-18-0483-R>
- Gent, D., Ocamb, C., & Farnsworth, A. (2013). Effect of pruning and inoculum removal on hop powdery mildew. *Plant Disease*, 97, 194–204. <https://doi.org/10.1094/PDIS-01-12-0084-RE>
- Gilligan, C. (2008). Sustainable agriculture and plant diseases: An epidemiological perspective. *Philosophical Transactions of the Royal Society B: Biological Sciences*, 363, 741–759. <https://doi.org/10.1098/rstb.2007.2181>
- Gilligan, C., Truscott, J., & Stacey, A. (2007). Impact of scale on the effectiveness of disease control strategies for epidemics with cryptic infection in a dynamical landscape: An example for a crop disease. *Journal of the Royal Society Interface*, 4, 925–934. <https://doi.org/10.1098/rsif.2007.1019>
- Hartfield, M., & Alizon, S. (2013). Introducing the outbreak threshold in epidemiology. *PLOS Pathogens*, 9(6), e1003277. <https://doi.org/10.1371/journal.ppat.1003277>
- Irwin, M. (1999). Implications of movement in developing and deploying integrated pest management strategies. *Agricultural and Forest Meteorology*, 97, 235–248. [https://doi.org/10.1016/S0168-1923\(99\)00069-6](https://doi.org/10.1016/S0168-1923(99)00069-6)
- Keeling, M., & Eames, K. (2005). Networks and epidemic models. *Journal of the Royal Society Interface*, 2, 295–307. <https://doi.org/10.1098/rsif.2005.0051>

- Lafontaine, S., & Shellhammer, T. (2015). How hoppy beer production and quality is influenced by dry hopping with pressed cones versus pellets. *PLoS ONE*, 10(4), e0120987. <https://doi.org/10.1371/journal.pone.0120987>
- Lence, S., & Singerman, A. (2022). When does voluntary coordination work? Evidence from area-wide pest management. *American Journal of Agricultural Economics*, 105, 243–264. <https://doi.org/10.1111/ajae.12308>
- Lofgren, E., Halloran, M., Rivers, C., Drake, J., Porco, T., Lewis, B., Yang, W., Vespignani, A., Shaman, J., Eisenberg, J., Eisenberg, M., Marathe, M., Scarpino, S., Alexander, K., Meza, R., Ferrari, M., Hyman, J., Meyers, L., & Eubank, S. (2014). Mathematical models: A key tool for outbreak response. *Proceedings of the National Academy of Sciences*, 111, 18095–18096. <https://doi.org/10.1073/pnas.1421551111>
- Mahaffee, W., & Stoll, R. (2016). The ebb and flow of airborne pathogens: Monitoring and use in disease management decisions. *Phytopathology*, 106, 420–431. <https://doi.org/10.1094/PHYTO-02-16-0060-RVW>
- Margosian, M., Garrett, K., Hutchinson, J., & With, K. (2009). Connectivity of the American agricultural landscape: Assessing the national risk of crop pest and disease spread. *BioScience*, 59, 141–151. <https://doi.org/10.1525/bio.2009.59.2.7>
- Marsh, T., Huffaker, R., & Long, G. (2000). Optimal control of vector-virus-plant interactions: The case of potato leafroll virus net necrosis. *American Journal of Agricultural Economics*, 82, 556–569. <https://doi.org/10.1111/0002-9092.00058>
- McDowell, R., Doherty, M., & Parker, W. (2018). Balancing water-quality threats from nutrients and production in agricultural catchments. *Journal of Applied Ecology*, 55, 2321–2333. <https://doi.org/10.1111/1365-2664.13144>
- Ojiambo, P., Gent, D., Mehra, L., Christie, D., & Magarey, R. (2017). Focus expansion and stability of the spread parameter estimate of the power law model for dispersal gradients. *PeerJ*, 5, e3465. <https://doi.org/10.7717/peerj.3465>
- Pastor-Satorras, R., & Vespignani, A. (2001). Epidemic spreading in scale-free networks. *Physical Review Letters*, 86, 3200–3203. <https://doi.org/10.1103/PhysRevLett.86.3200>
- Pautasso, M., Moslonka-Lefebvre, M., & Jeger, M. (2010). The number of links to and from the starting node as a predictor of epidemic size in small-size directed networks. *Ecological Complexity*, 7, 94–101. <https://doi.org/10.1016/j.ecocom.2009.10.003>
- Pimentel, D. (2005). Environmental and economic costs of the application of pesticides primarily in the United States. *Environmental Development and Sustainability*, 7, 229–252. <https://doi.org/10.1007/s10668-005-7314-2>
- Severns, P., Estep, L., Sackett, K., & Mundt, C. (2014). Degree of host susceptibility in the initial disease outbreak influences subsequent epidemic spread. *Journal of Applied Ecology*, 51, 1622–1630. <https://doi.org/10.1111/1365-2664.12326>

- Severns, P., & Mundt, C. (2022). Delays in epidemic outbreak control cost disproportionately large treatment footprints to offset. *Pathogens*, 11, 393. <https://doi.org/10.3390/pathogens11040393> 789  
790  
791
- Severns, P., Sackett, K., Farber, D., & Mundt, C. (2019). Consequences of long-distance dispersal for epidemic spread: Patterns, scaling, and mitigation. *Plant Disease*, 103, 177–191. <https://doi.org/10.1094/PDIS-03-18-0505-FE> 792  
793  
794
- Thompson, R., Cobb, R., Gilligan, C., & Cunniffe, N. (2016). Management of invading pathogens should be informed by epidemiology rather than administrative boundaries. *Ecological Modelling*, 324, 28–32. <https://doi.org/10.1016/j.ecolmodel.2015.12.014> 795  
796  
797  
798
- van der Plank, J. (1963). *Plant diseases: Epidemics and control*. Academic Press. 799
- Xu, X.-M., & Ridout, M. (1998). Effects of initial epidemic conditions, sporulation rate, and spore dispersal gradient on the spatio-temporal dynamics of plant disease epidemics. *Phytopathology*, 88, 1000–1012. <https://doi.org/10.1094/PHYTO.1998.88.10.1000> 800  
801  
802  
803

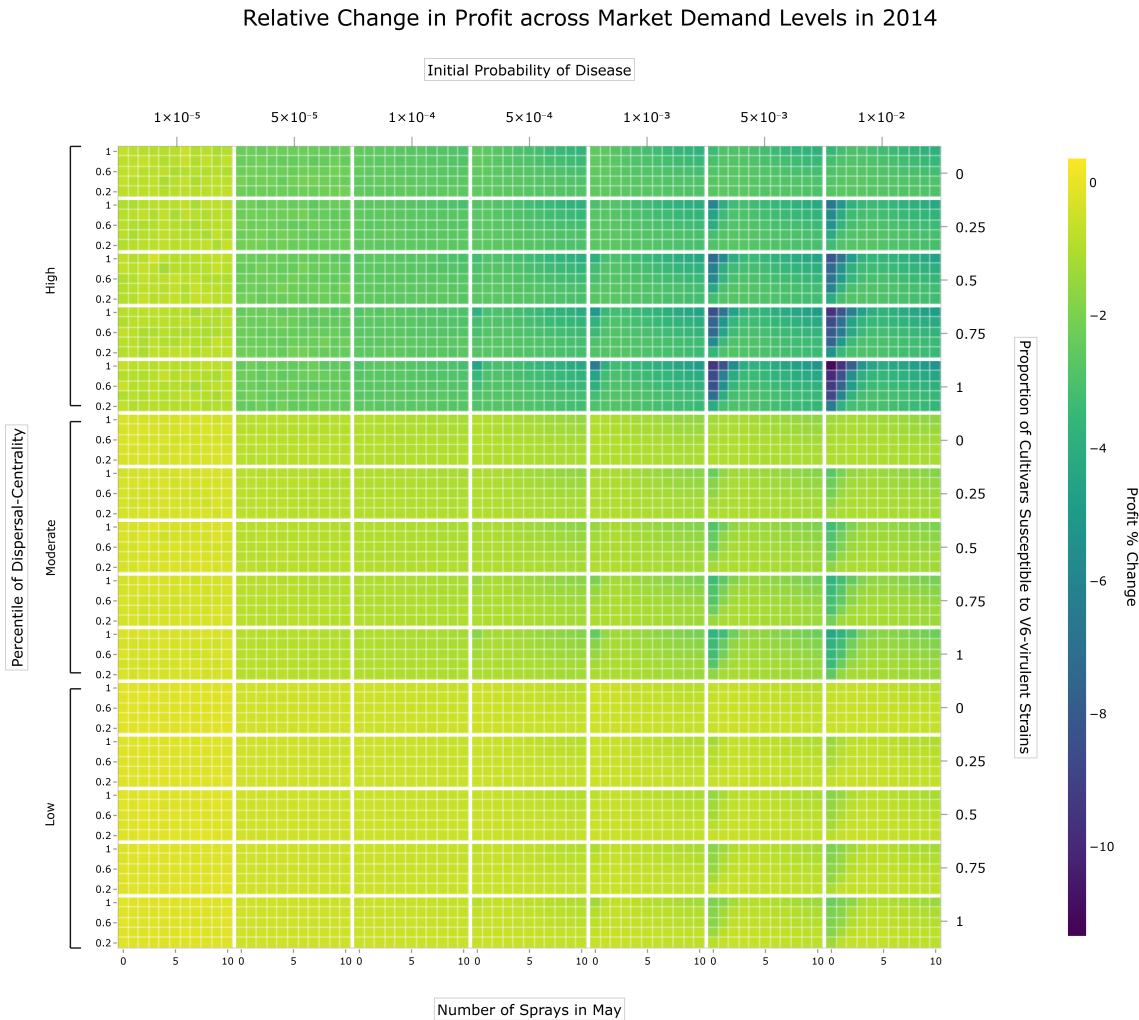


**Figure 6: Relative change in profit for high, moderate, and low market demand in 2014.** This comprehensive heatmap shows the profit percentage change across different initial probability of disease ( $p_0$ ) values (rows), number of sprays in May (columns), and percentile of dispersal-centrality (panels within each market scenario) for varying V6 percentages (0%, 25%, 50%, 75%, 100%) under three market demand scenarios (high, moderate, low). Yellow indicates minimal profit impact, while dark blue/purple represents substantial profit losses. The visualization demonstrates how market conditions affect the optimal control strategies for hop powdery mildew management.

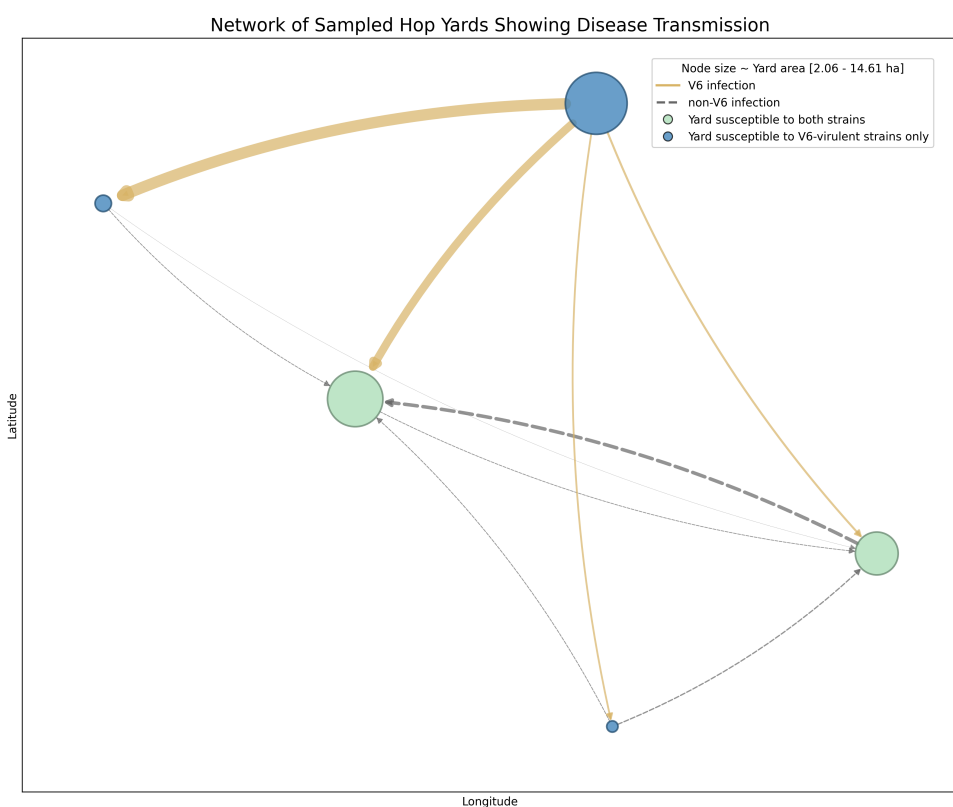


Figure 7: Network visualization of hop yard connectivity for epidemic modeling. Nodes represent individual hop yards with size proportional to yard acreage and color indicating degree centrality. Edge connections represent potential pathogen transmission pathways based on distance and wind patterns. This network structure underlies the spatial epidemic simulations described in the Methods section.

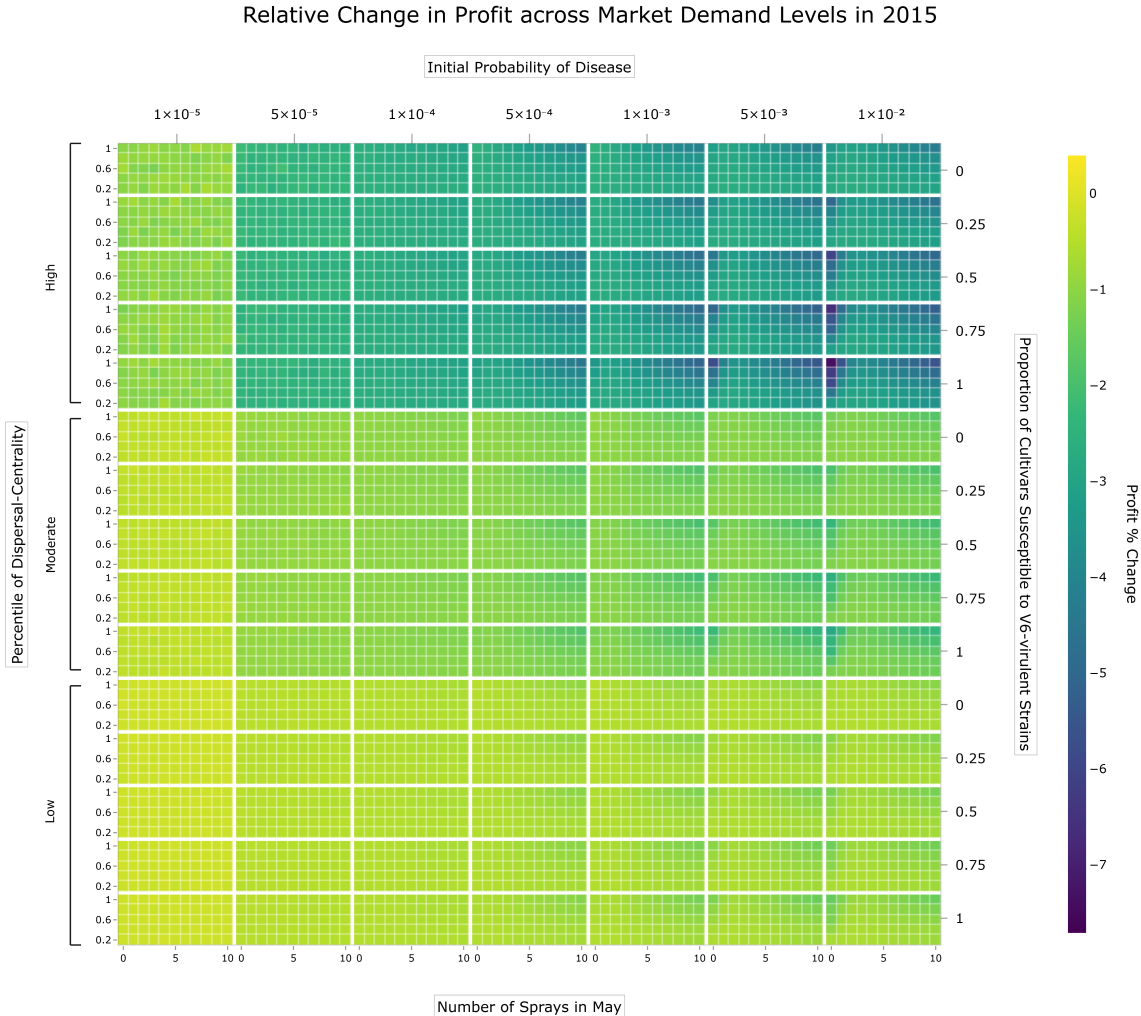


Figure 8: Relative Change in Profit for High, Moderate, and Low Market Demand in 2015. This heatmap shows the profit percentage change across different initial probability of disease ( $p_0$ ) values, number of sprays in May, and percentile of dispersal-centrality for varying V6 percentages (0%, 25%, 50%, 75%, 100%) under three market demand scenarios. The visualization demonstrates how market conditions affect the optimal control strategies for hop powdery mildew management in 2015, showing similar patterns to 2014 but with year-specific variations in yard layout and weather conditions.

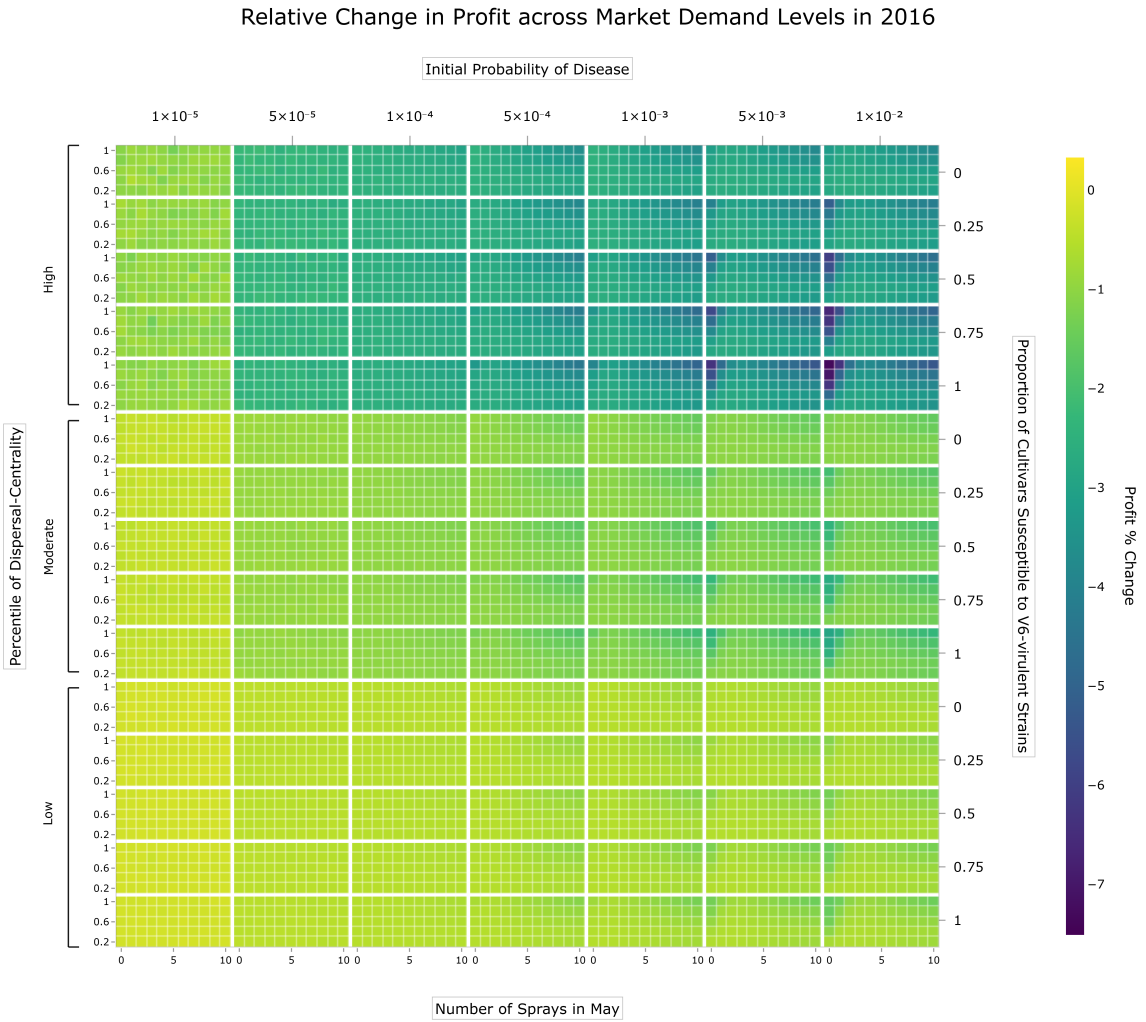


Figure 9: Relative Change in Profit for High, Moderate, and Low Market Demand in 2016. This heatmap shows the profit percentage change across different initial probability of disease ( $p_0$ ) values, number of sprays in May, and percentile of dispersal-centrality for varying V6 percentages (0%, 25%, 50%, 75%, 100%) under three market demand scenarios. The visualization demonstrates how market conditions affect the optimal control strategies for hop powdery mildew management in 2016, reflecting the impact of that year's specific environmental and spatial conditions.

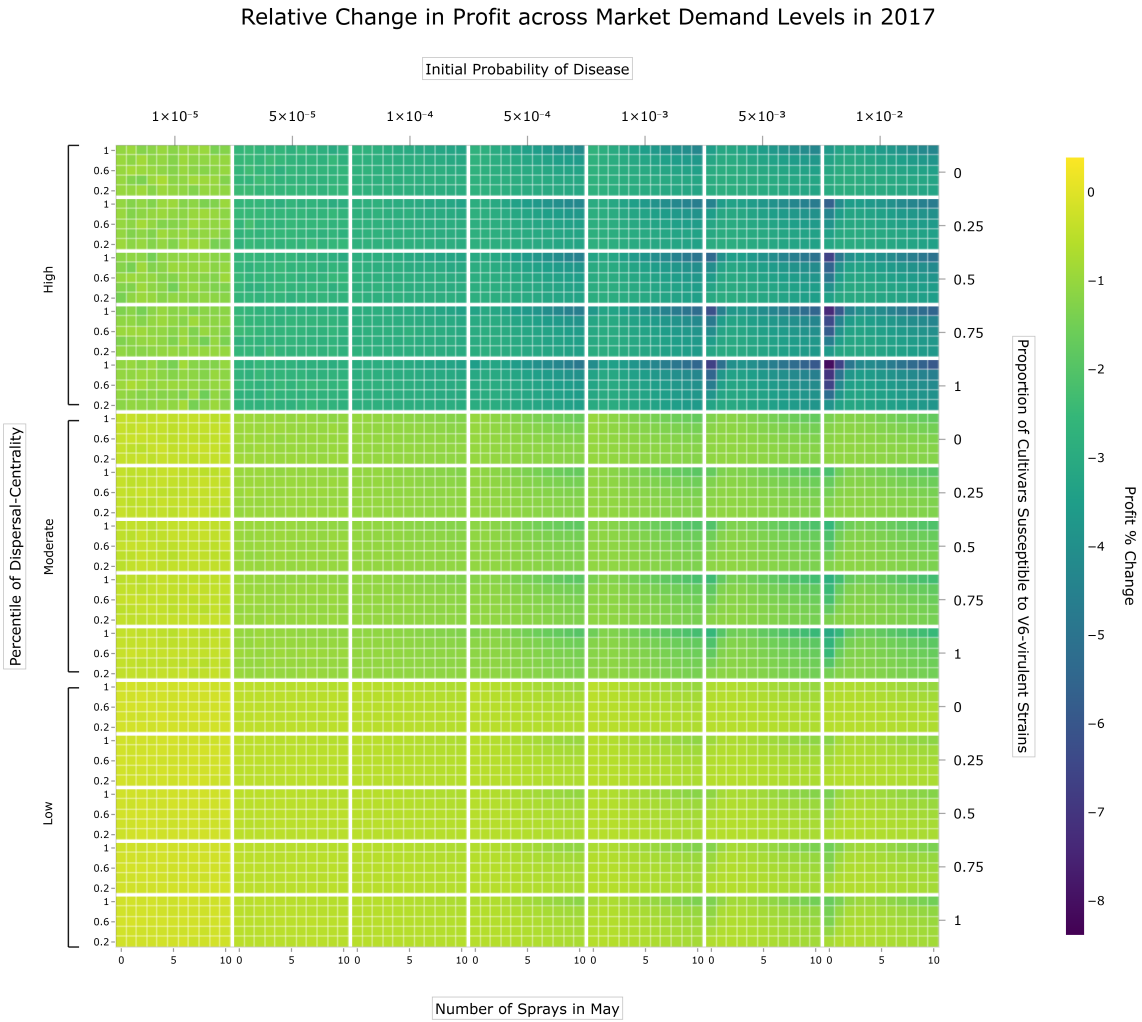


Figure 10: Relative Change in Profit for High, Moderate, and Low Market Demand in 2017. This heatmap shows the profit percentage change across different initial probability of disease ( $p_0$ ) values, number of sprays in May, and percentile of dispersal-centrality for varying V6 percentages (0%, 25%, 50%, 75%, 100%) under three market demand scenarios. The visualization demonstrates how market conditions affect the optimal control strategies for hop powdery mildew management in 2017, completing the four-year analysis period and showing consistent patterns across years despite inter-annual variability.